nature microbiology

LETTERS

https://doi.org/10.1038/s41564-018-0151-5

A high-frequency phenotypic switch links bacterial virulence and environmental survival in *Acinetobacter baumannii*

Chui Yoke Chin[1,2,3,4,8], Kyle A. Tipton[5,8], Marjan Farokhyfar[6], Eileen M. Burd[3,4,7], David S. Weiss[1,2,3,4,6*] and Philip N. Rather[4,5,6*]

Antibiotic-resistant infections lead to 700,000 deaths per year worldwide[1]. The roles of phenotypically diverse subpopulations of clonal bacteria in the progression of diseases are unclear. We found that the increasingly pathogenic and antibiotic-resistant pathogen *Acinetobacter baumannii* harbours a highly virulent subpopulation of cells responsible for disease. This virulent subpopulation possesses a thicker capsule and is resistant to host antimicrobials, which drive its enrichment during infection. Importantly, bacteria harvested from the bloodstream of human patients belong exclusively to this virulent subpopulation. Furthermore, the virulent form exhibits increased resistance to hospital disinfectants and desiccation, indicating a role in environmental persistence and the epidemic spread of disease. We identified a transcriptional 'master regulator' of the switch between avirulent and virulent cells, the overexpression of which abrogates virulence. Furthermore, the overexpression strain is capable of vaccinating mice against lethal challenge. This work highlights a phenotypic subpopulation of bacteria that drastically alters the outcome of infection, and illustrates how knowledge of the regulatory mechanisms controlling such phenotypic switches can be harnessed to attenuate bacteria and develop translational interventions.

Acinetobacter baumannii has become a major healthcare threat worldwide, responsible for both hospital- and community-acquired infections[2–6]. These infections have become increasingly virulent[7–10] and exceedingly difficult to treat due to high levels of antibiotic resistance (63% of isolates in the United States are multidrug-resistant, and some isolates are even pan-resistant)[11–15]. *A. baumannii* is also notoriously difficult to eradicate in hospital settings[2,14] and contamination of intensive care wards is a frequent problem[6,16,17]. The remarkable ability of *A. baumannii* to persist in this environment is due to both its intrinsic resistance to commonly used disinfectants and its ability to survive long periods of desiccation[18–21]. However, the molecular mechanisms controlling virulence, resistance to disinfectants and desiccation tolerance remain poorly understood.

Bacteria can exhibit genotypic and/or phenotypic heterogeneity. Phenotypic heterogeneity concerns traits expressed by some cells within a genetically homogenous population. Characterization of the highly virulent *A. baumannii* isolate AB5075 (ref. [22]) revealed that it exhibits phenotypic heterogeneity by rapidly interconverting between cells capable of forming opaque or translucent colonies[23] (Fig. 1a). A single colony can be sequentially propagated between opaque and translucent states with switching frequencies of ~4–13% in 24 h colonies (Supplementary Fig. 1) and 20–40% in 48 h colonies (Supplementary Fig. 2). We hypothesized that differences in capsule contributed to the opacity differences between virulent opaque (VIR-O) and avirulent translucent (AV-T) cells. Examination of cells by electron microscopy after staining for capsule with ruthenium red revealed that VIR-O cells produce a capsule with a two-fold increased thickness compared with AV-T cells (Fig. 1b,c). In comparison, VIR-O and AV-T cells missing the Wzc tyrosine kinase required for capsule synthesis (*Δwzc*) failed to produce any capsular material and exhibited a translucent phenotype that was more pronounced than in AV-T cells[24].

The role of these two phenotypic subpopulations in the progression of disease was unclear. After intranasal inoculation of mice with a 1:1 mixture of the two types of cells, VIR-O cells vastly outcompeted AV-T cells in all organs tested (that is, the lungs, spleen and liver) at 24 h post-infection (Fig. 1d). Similar results were obtained in single-infection experiments where mice infected with VIR-O cells harboured over 10,000-fold more bacteria in the lungs than mice infected with AV-T cells (Fig. 1e). In addition, 1,000-fold more bacteria were recovered in the spleens and livers of the VIR-O-infected mice than those infected with AV-T cells (Supplementary Fig. 3). Surprisingly, while bacteria recovered from VIR-O-infected mice remained in the VIR-O form (Fig. 1f), there was a greater than 3,000-fold increase in the frequency of VIR-O cells recovered from the AV-T-infected mice compared with the inoculum (0.01% VIR-O cells in the inoculum of AV-T-infected mice) (Fig. 1g). Furthermore, VIR-O cells derived from AV-T colonies regained virulence in mice (Supplementary Fig. 4), confirming that the attenuation of AV-T cells was not due to random mutations within the genome. These results reveal a strong selective pressure for the VIR-O population in vivo. In survival experiments, VIR-O-infected mice rapidly succumbed to disease by day 2, whereas AV-T-infected mice survived (Fig. 1h). VIR-O and AV-T variants exhibited similar growth rates in both rich and defined media, indicating that intrinsic growth rate differences do not account for the virulence defect of AV-T variants (Supplementary Fig. 5). Taken together, these data

[1]Emory Vaccine Center, Emory University School of Medicine, Atlanta, GA, USA. [2]Yerkes National Primate Research Center, Emory University School of Medicine, Atlanta, GA, USA. [3]Division of Infectious Diseases, Department of Medicine, Emory University School of Medicine, Atlanta, GA, USA. [4]Emory Antibiotic Resistance Center, Emory University School of Medicine, Atlanta, GA, USA. [5]Department of Microbiology and Immunology, Emory University School of Medicine, Atlanta, GA, USA. [6]Research Service, Atlanta VA Medical Center, Decatur, GA, USA. [7]Department of Pathology and Laboratory Medicine, Emory University, Atlanta, GA, USA. [8]These authors contributed equally: Chui Yoke Chin and Kyle A. Tipton.
*e-mail: david.weiss@emory.edu; prather@emory.edu

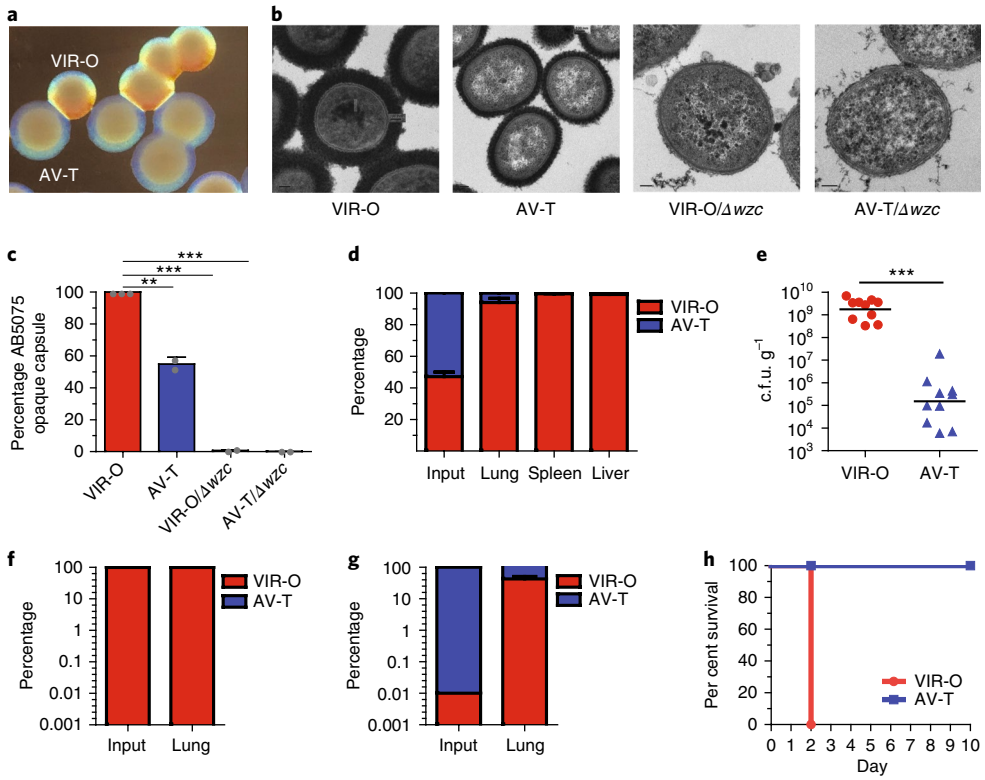

Fig. 1 | A highly VIR-O population is responsible for causing disease during in vivo pulmonary infection of mice. a, Representative *A. baumannii* strain AB5075 WT VIR-O and AV-T colonies. **b**, Strains were stained for capsule with ruthenium red and imaged by transmission electron microscopy. Representative images are shown for each strain. Scale bars, 100 nm. **c**, Capsule abundance of the indicated strains was determined by capsule extraction and quantitation on sodium dodecyl sulphate polyacrylamide gel electrophoresis gels stained with Alcian blue. Values were obtained from three biological replicates and error bars represent s.d. of the mean. *P* values (**$P < 0.005$; ***$P < 0.0005$) were determined using one-way ANOVA. **d**, Mice were infected with a 1:1 mixture of VIR-O (red) and AV-T (blue) strains ($n = 5$ per group). At 24 h post-infection, organs were harvested and plated to assess the percentage of VIR-O and AV-T cells present. **e**, Mice were infected with VIR-O and AV-T ($n = 5$ per group). The presented data were pooled from two separate experiments and repeated at least ten times. At 24 h post-infection, lungs were harvested and plated for c.f.u. Bars represent the geometric mean and significance was determined using a two-tailed Mann–Whitney test (***$P < 0.0005$). **f**,**g**, Bacteria recovered from the VIR-O (**f**) and AV-T-infected lungs (**g**) were assessed for the percentage of VIR-O and AV-T cells present, respectively. **h**, Survival of mice infected with VIR-O and AV-T ($n = 5$ per group). This experiment was repeated three times. Error bars represent s.d. of the mean in **d**, **f** and **g**.

indicate that the VIR-O population is virulent and predominates during in vivo infection, whereas the AV-T population is unable to cause acute disease.

It was unclear which factors were responsible for the enrichment of the VIR-O population following in vivo lung infection (Fig. 1e). The lung is replete with innate immune antimicrobials including lysozyme, antimicrobial peptides such as cathelicidin-related antimicrobial peptide (CRAMP), and reactive oxygen species[25,26]. We hypothesized that VIR-O cells might be more resistant than AV-T cells to such antimicrobials. To test this, we conducted time-kill assays with hydrogen peroxide (which leads to the generation of reactive oxygen species), lysozyme and CRAMP. After 1 h of treatment with each of the three antimicrobials, VIR-O cells vastly outnumbered AV-T cells (Fig. 2a). Moreover, VIR-O cells also outnumbered AV-T after treatment with LL-37—the human orthologue of CRAMP (Supplementary Fig. 6). These data highlight that VIR-O cells are more resistant than AV-T cells to diverse innate immune antimicrobials.

To test whether these host defences contributed to the enrichment of the VIR-O subpopulation during in vivo infection, wild-type (WT) mice and triple knockout (TKO) mice lacking a functional reduced nicotinamide adenine dinucleotide phosphate (NADPH) oxidase (*cybb*$^{-/-}$; required for the production of reactive oxygen species), CRAMP (*cramp*$^{-/-}$) and lysozyme (*lysM*$^{-/-}$) were infected with an inoculum of AV-T cells. At 8 h post-infection, lungs from WT mice harboured a higher percentage of VIR-O cells compared with TKO mice (Fig. 2b). This was despite the overall levels of bacteria being higher in TKO mice than WT mice (Supplementary Fig. 7). These data indicate that reactive oxygen species, CRAMP and lysozyme specifically contribute to the enrichment of the virulent VIR-O subpopulation during early infection. However, since the VIR-O population was still enriched in TKO mice, this indicates that other host factors are involved as well.

Since the VIR-O subpopulation displayed increased resistance to host-derived antimicrobials, we hypothesized that the cells might also exhibit resistance to hospital disinfectants. The VIR-O and AV-T subpopulations were tested for sensitivity to three of the most commonly used disinfectants—benzethonium chloride (BZT), benzalkonium chloride (BAK) and chlorhexidine gluconate (CHG)—and the VIR-O cells displayed increased resistance to all three agents compared with the AV-T cells (Fig. 2c–e). In addition to resistance to disinfectants, desiccation resistance is a major contributor to the persistence of *A. baumannii* in the hospital environment. Following eight days of desiccation, VIR-O cells survived better on dry surfaces compared with AV-T cells (Fig. 2f). Moreover, while viable bacteria recovered from VIR-O cells remained in the VIR-O form (Fig. 2g), there was a greater than 5,000-fold increase in the frequency of VIR-O cells recovered from the desiccated AV-T cells

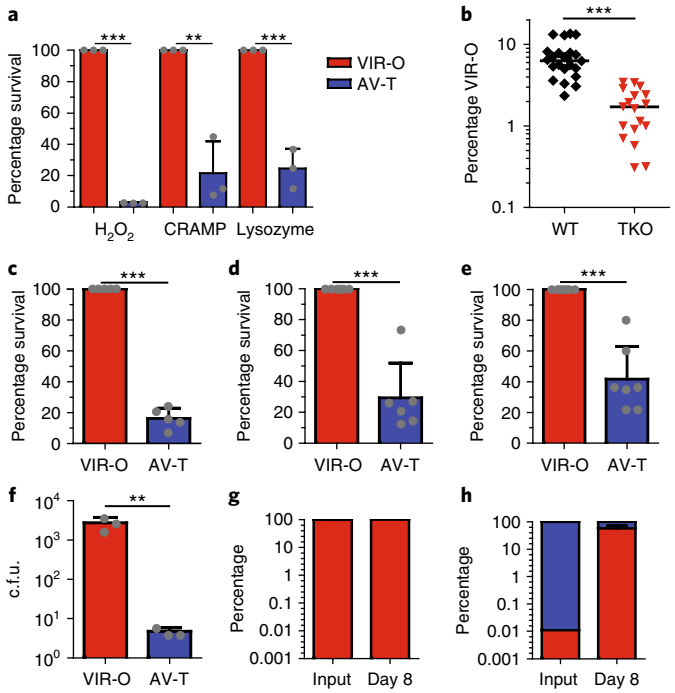

Fig. 2 | Host antimicrobial, and hospital-disinfectant- and desiccation-resistant VIR-O cells are selected during in vivo infection. a, VIR-O (red) or AV-T cells (blue) were treated with H_2O_2, CRAMP or lysozyme, and the percentage survival relative to VIR-O was calculated. Reported values represent the mean of three replicates and s.d. Repeated experiments gave similar results. **b**, WT (black) or TKO (red) mice lacking the gp91 subunit of NADPH oxidase, lysozyme and CRAMP were infected with AV-T ($n = 4$–8 per group). At eight hours post-infection, lungs were harvested and plated to assess the percentage of VIR-O cells present. Presented data were pooled from 3 separate experiments and repeated at least 5 times for a total of 18–23 mice per group. **c**–**e**, VIR-O or AV-T cells were treated with disinfectants (BZT 0.01% (**c**), BAK 0.004% (**d**) or CHG 0.008% (**e**)) and percentage survival relative to VIR-O was calculated. The presented data were pooled from three separate experiments and a total of five, six and seven replicates were used for **c**, **d** and **e**, respectively. **f**–**h**, VIR-O and AV-T survival after desiccation. Bacteria were rehydrated and plated on day 8 of desiccation to determine viability (**f**). Values represent the mean of three replicates. Recovered bacteria from the VIR-O (**g**) and AV-T cells (**h**) were assessed to determine the percentage of VIR-O and AV-T cells present. In **a** and **c**–**h**, error bars represent s.d. of the mean and *P* values (**$P < 0.005$; ***$P < 0.0005$) were calculated by Student's two-tailed *t*-test. In **b**, bars represent the geometric mean and the *P* value (***$P < 0.0005$) was calculated by two-tailed Mann–Whitney test.

(Fig. 2h). Taken together, these data link increased virulence and environmental persistence (resistance to hospital disinfectants and desiccation) to a single phenotypic subpopulation of bacterial cells.

To elucidate factors controlling the VIR-O and AV-T subpopulations, we performed genome-wide transcriptional profiling using RNA sequencing (RNA-Seq). This revealed that a predicted TetR-type transcriptional regulator, *ABUW_1645*, was among the most differentially expressed regulatory genes between the VIR-O and AV-T subpopulations (Supplementary Table 1). Quantitative real-time polymerase chain reaction (PCR) confirmed that the AV-T population expressed 60-fold higher levels of *ABUW_1645* compared with VIR-O cells (Supplementary Fig. 8). Intriguingly, *ABUW_1645* expression was reduced significantly as AV-T cells gradually switched to VIR-O (Supplementary Fig. 9a), whereas its expression level in VIR-O cells remained low (Supplementary Fig. 9b). An in-frame deletion of *ABUW_1645* did not alter the rate of VIR-O to AV-T switching, but the rate of AV-T to VIR-O switching was increased 18-fold relative to WT, indicating a role for *ABUW_1645* in maintaining the AV-T state (Supplementary Fig. 10).

Strikingly, overexpression of *ABUW_1645* in VIR-O cells (VIR-O/1645) led to a translucent colony morphology and a complete inability to switch back to VIR-O (Fig. 3a). AV-T cells overexpressing *ABUW_1645* (AV-T/1645) were similarly 'locked' and unable to switch to VIR-O cells (Fig. 3a). Transcriptional profiling of VIR-O/vector and VIR-O/1645 cells revealed that *ABUW_1645* controlled ~70% of the genes differentially expressed between the VIR-O and AV-T cells (Supplementary Table 1). Taken together, these data identify *ABUW_1645* as a key regulator of the VIR-O/AV-T high-frequency phenotypic switch.

Previously identified mutations that either increased (*ompR*)[27] or decreased (*arpB*)[28] the rate of VIR-O to AV-T switching did not alter *ABUW_1645* expression (Supplementary Fig. 11a). Furthermore, the *ABUW_1645* deletion did not alter the hyper-switching phenotype of an *ompR::Tc* mutant (Supplementary Fig. 11b). In addition, RNA-Seq data indicated that the expression of *ompR* or *arpB* was not altered by *ABUW_1645* overexpression (Supplementary Table 1). Therefore, *ABUW_1645* regulates phenotypic switching by a pathway separate from that regulated by OmpR or ArpB.

Overexpression of *ABUW_1645* in VIR-O cells completely reversed resistance to host antimicrobials (Fig. 3b), disinfectants (Supplementary Fig. 12a,b) and desiccation (Supplementary Fig. 12c,d). In single-infection experiments, VIR-O cells were recovered from mice infected with either VIR-O/vector or AV-T/vector cells (Fig. 3c). In contrast, only AV-T cells were recovered from mice infected with *ABUW_1645* overexpression strains (Fig. 3c). This was associated with drastic attenuation of both VIR-O/1645 and AV-T/1645 strains, which exhibited a 7-log reduction in bacterial levels in the lungs relative to VIR-O/vector-infected mice (Fig. 3d). Furthermore, since the *ABUW_1645* overexpression strains were even less virulent than AV-T cells, these data indicate that the residual colonization of mice during AV-T infection was in fact due to VIR-O cells, which become enriched during infection. This strongly indicates that AV-T cells do not have the ability to replicate and/or survive during in vivo infection, whereas VIR-O cells are responsible for causing disease. In agreement with these findings, infection of mice with the *ABUW_1645* deletion mutant led to the recovery of VIR-O cells. This strain was not attenuated compared with the WT (Supplementary Fig. 13), but the *ABUW_1645* overexpression strain was. VIR-O/1645 bacteria were unable to cause a lethal infection, whereas VIR-O/vector cells caused a rapidly lethal infection (Fig. 3e). These data highlight *ABUW_1645* as a critical regulator of virulence, as well as traits associated with persistence in the hospital environment.

Since the VIR-O/1645 strain was completely attenuated in vivo, we tested whether it might protect mice against subsequent lethal challenge with the virulent VIR-O/vector cells. While control mice vaccinated with phosphate buffered saline (PBS) or *Escherichia coli* K-12 rapidly succumbed to challenge on day 2, mice vaccinated with VIR-O/1645 were completely protected (Fig. 3f). These data demonstrate that a strain engineered to be locked to produce only avirulent cells can effectively provide protection against otherwise lethal infection, serving as a live-attenuated vaccine against *A. baumannii*.

Because VIR-O cells clearly predominate during experimental in vivo murine infection, as well as in conditions that simulate stresses encountered in the hospital environment, we set out to test their abundance in samples from hospitalized human patients. Blood cultures from five patients with systemic *A. baumannii* infections were directly plated on agar and only VIR-O cells were detected from these clinical isolates (Fig. 3g). Therefore, similar to experimental infections in mice, VIR-O cells vastly predominate in human

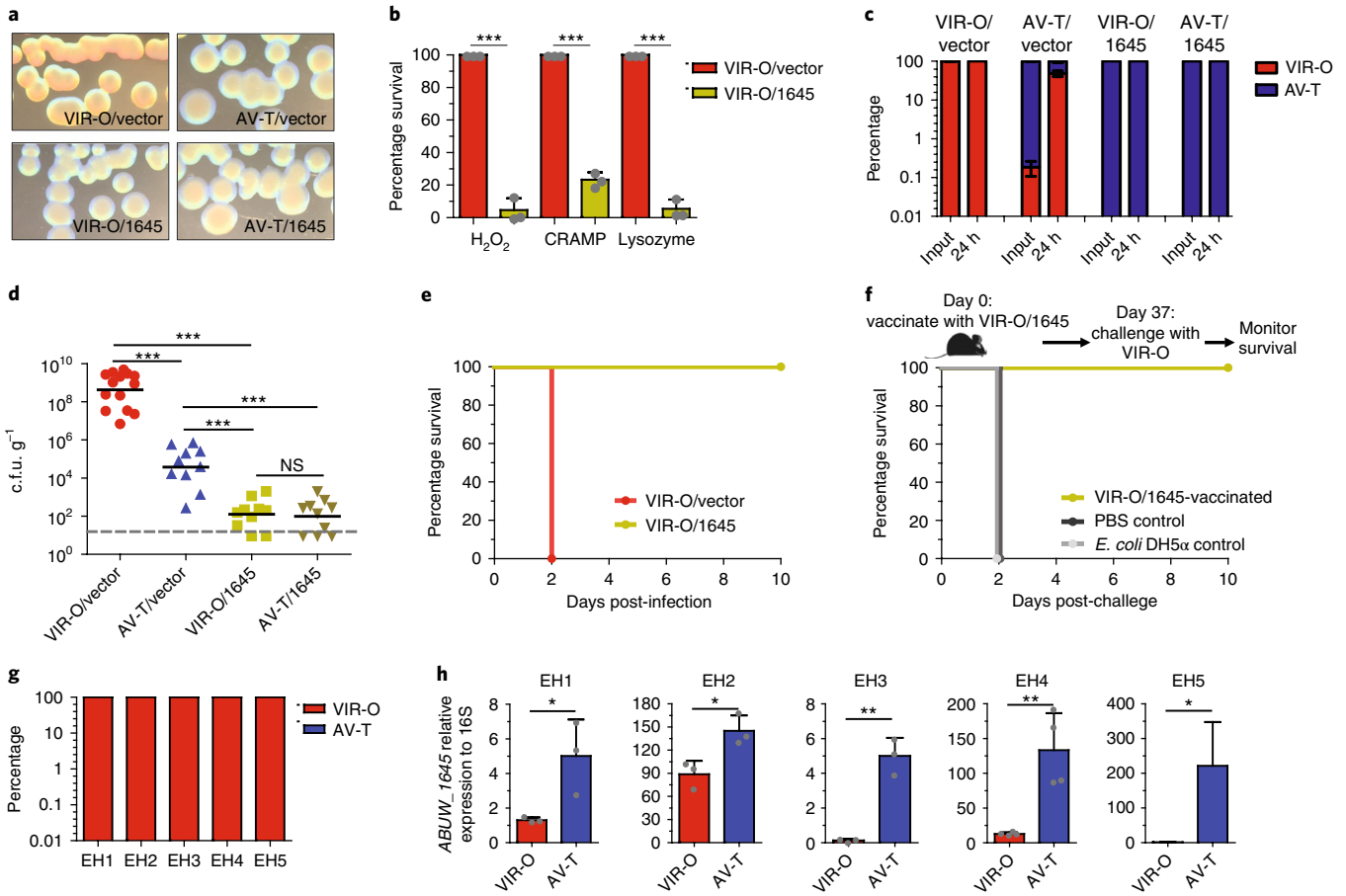

Fig. 3 | *ABUW_1645* is a global regulator in mediating phenotypic switching, virulence and resistance to host defences. a, Representative colonies of VIR-O or AV-T cells overexpressing *ABUW_1645* or with empty vector. **b**, VIR-O/vector (red) and VIR-O/1645 (green) were treated with lysozyme, H_2O_2 or CRAMP, and percentage survival relative to the VIR-O/vector was calculated. The reported values represent the mean and s.d. of three independent replicates. Repeated experiments gave similar results. **c**,**d**, Mice were infected with VIR-O/vector (red), AV-T/vector (blue), VIR-O/1645 (green) or AV-T/1645 (gold) strains ($n=10$ per group). At 24 h post-infection, lungs were harvested and plated for c.f.u. (**d**) and assessed for the percentage of VIR-O and AV-T cells present (**c**). **e**, Survival of mice infected with VIR-O/vector versus VIR-O/1645 ($n=5$ per group). This experiment was repeated twice with identical results. **f**, Survival of VIR-O/1645- and *E. coli*-vaccinated mice after lethal challenge ($n=5$ per group). This experiment was repeated twice with identical results. **g**, Blood cultures from *A. baumannii*-infected patients (EH1–5) were plated directly on 0.5× LB agar plates to assess the percentage of VIR-O and AV-T cells present. **h**, For each isolate (EH1–5), AV-T variants were isolated from the VIR-O colonies and the expression of *ABUW_1645* was determined in each variant by quantitative real-time PCR. Data represent the mean from three replicates and error bars represent s.d. from the mean. A Student's two-tailed *t*-test (*$P<0.05$; **$P<0.005$; ***$P<0.0005$) was used in **b** and **h**. A two-tailed Mann–Whitney test (***$P<0.0005$) was used in **d**. NS, not significant.

infections. In addition, AV-T variants could be selected from the VIR-O cells of each clinical isolate, indicating that this phenotypic switch is present in *A. baumannii* isolates other than AB5075. Moreover, the expression of *ABUW_1645* was significantly higher in the AV-T subpopulation from each isolate, relative to the corresponding VIR-O subpopulation, further supporting the key role of this regulator in the VIR-O to AV-T switch (Fig. 3h). These results provide clinical evidence from diverse isolates that highlights the critical role of the phenotypic subpopulation of VIR-O cells in human disease.

A remaining question is: what advantages does the AV-T subpopulation confer to *A. baumannii*? A subset of genes upregulated in the AV-T cells are predicted to be involved in the catabolism of aromatic compounds (*ABUW_0066*, *ABUW_0068* and *ABUW_0070*), generation of free phosphate and sulphur from organic sources (*ABUW_0904* and *ABUW_2921*), iron storage (*ABUW_3125*) and nutrient transport (*ABUW_0143*, *ABUW_3403* and *ABUW_1660*). This raises the possibility that the AV-T subpopulation is better suited for natural environments outside the host, where nutrients are limited and bacteria may rely on the uptake and catabolism of atypical compounds for use as nutrients. Indeed, AV-T cells grew to higher yields in a nutrient poor media (Chamberlain's) relative to VIR-O cells (Fig. 4a). Biofilm formation may facilitate colonization of natural environments, such as in soil and water, and AV-T cells were shown to be more proficient than VIR-O cells at biofilm formation at low temperature (25 °C) (Fig. 4b). Furthermore, at low temperature outside the host, *ABUW_1645* expression in AV-T cells was increased and was subsequently reduced in cells grown at 37 °C (Fig. 4c). Correspondingly, when AV-T cells were grown at the host temperature (37 °C), as would occur during infection, their rate of switching to VIR-O cells increased more than 3,400-fold (Fig. 4d). These data are in agreement with those from mouse infections (Fig. 1) and human samples (Fig. 3), in which VIR-O cells vastly outnumber AV-T cells. Taken together, these results suggest that AV-T cells are better suited to survive in certain environmental conditions, and their reduced levels of capsule may even render these cells resistant to bacteriophages[29].

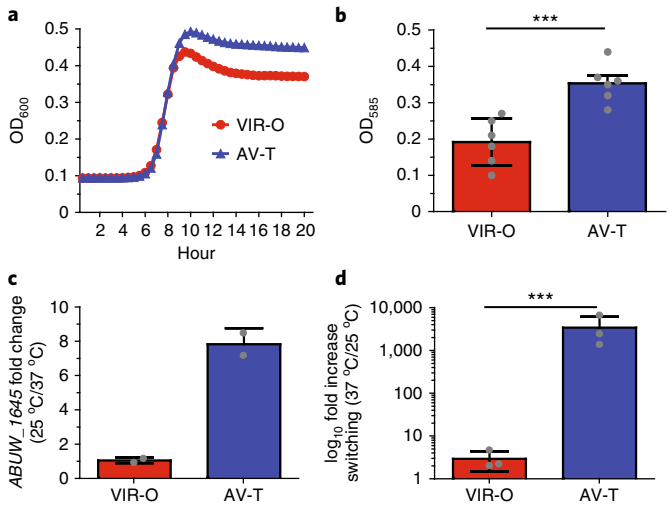

Fig. 4 | AV-T-specific phenotypes. a, Growth curves of VIR-O and AV-T in Chamberlain's minimal media. A representative experiment is shown, and repeated experiments gave similar results. **b**, Biofilm formation of VIR-O and AV-T cells grown for 24 h at 25 °C. Values represent the average of six replicates for each strain. A Student's two-tailed *t*-test was used to determine significance (***$P < 0.0005$). **c**, Ratio of *ABUW_1645* expression in VIR-O and AV-T cells at low (25 °C) and high temperature (37 °C). Values represent the averages of two independent biological replicates. **d**, Phenotypic switching of VIR-O and AV-T cells at low (25 °C) and high temperature (37 °C) in LB media harvested at an OD_{600} of 1.6. Values represent three biological replicates. A two-tailed paired *t*-test (***$P < 0.001$) was used to determine significance. Error bars in panels **b**–**d** represent s.d.

This study reveals a phenotypic switch linking resistance to host antimicrobials, virulence and environmental persistence. The data highlight an unexpected role for specific host innate immune antimicrobials (CRAMP, lysozyme and H_2O_2) in enriching the virulent VIR-O subpopulation during murine infection. Our data clearly demonstrate that VIR-O cells are responsible for causing disease in vivo. In addition to being the predominant cells recovered from infected mice, only VIR-O cells were found in the bloodstream of infected human patients, highlighting their critical role in virulence. It is therefore likely that the bacterial cells shed into the environment by infected patients are in the VIR-O form. Interestingly, VIR-O cells also have an increased ability to resist disinfectants and desiccation—two stresses encountered in the hospital environment. This suggests that, alarmingly, human infection selects for cells that are best-suited for environmental persistence and that, likewise, the bacterial cells persisting in the environment are those that are most virulent when transmitted to future human hosts. Therefore, the VIR-O subpopulation probably underlies a worrisome cycle present in hospital wards, accounting for the difficulty in eradicating *A. baumannii* as well as the high virulence of many of these infections.

Phenotypic switches that control virulence have been identified in both bacterial and fungal pathogens and this may also represent a bet-hedging strategy where the avirulent subpopulation has a selective advantage outside the host[30–35]. Interestingly, a phenotypic switch in *Photorhabdus luminescens* has similarities to *A. baumannii*, where a virulent subpopulation is more resistant to host antimicrobials[34]. In addition, in the eukaryote *Candida albicans*, a phenotypic switch that controls the white–opaque colony transition also has parallels with the *A. baumannii* system, including subpopulation differences in virulence, cell shape and biofilm formation[35].

Overexpression of *ABUW_1645* completely converted VIR-O cells to AV-T cells, and reversed the virulence and environmental persistence attributes of VIR-O cells (Fig. 3). Thus, while the VIR-O/AV-T phenotypic switch is critical for facilitating *A. baumannii* virulence, our data suggest that it could be subverted and turned into an 'Achilles' heel'. Small molecules that drive cells into the AV-T form would render cells avirulent and could represent a potential therapeutic approach for the treatment of infections. Furthermore, we demonstrate that the highly attenuated *ABUW_1645* overexpression strain is a promising live-attenuated vaccine candidate against *A. baumannii*, exerting striking protection against lethal challenge. These findings highlight how knowledge of phenotypic traits endowed by subpopulations of cells can be harnessed to facilitate translational interventions.

Methods

Bacterial strains. *A. baumannii* strain AB5075 was used in this study. All experiments were performed using the same glycerol stock of VIR-O and AV-T cells that were at least 99.9% pure. For each mouse infection, the bacterial inoculum was checked to verify that each culture maintained the VIR-O or AV-T phenotype. *E. coli* strain EC100D (Epicentre) was used for all cloning experiments.

Methods to distinguish VIR-O and AV-T variants. The ability to distinguish between VIR-O and AV-T variants requires the use of a stereo (dissecting) microscope that illuminates the plates from below using a light source with an adjustable angle (oblique lighting). A correct light angle is required to observe the opacity differences and an improper light angle can make opaque colonies look transparent and vice-versa. Each microscope should be standardized with VIR-O and AV-T variants to set the proper angle. VIR-O and AV-T stocks will be made available upon request. Colonies should be grown on agar plates composed of 5 g l^{-1} tryptone, 2.5 g l^{-1} yeast extract, 2.5 g l^{-1} sodium chloride and 8 g l^{-1} agar (0.5× lysogeny broth (LB)/0.8% agar). The VIR-O and AV-T phenotypes can be observed on regular LB plates, but it is much harder to distinguish the variants. Importantly, the VIR-O and AV-T opacity phenotypes can only be accurately distinguished at high colony density (~100 plate^{-1}). At low colony density, both variants look like VIR-O. In addition, VIR-O colonies typically give rise to translucent sectors after 24 h. AV-T colonies rarely sector to VIR-O, yet AV-T colonies can have up to 50% VIR-O cells at 48 h.

Electron microscopy. Colonies of bacteria were collected from culture plates and placed in 0.1 M sodium cacodylate (pH 7.4) buffered fixative that contained 2% paraformaldehyde, 2.5% glutaraldehyde, 0.075 g of ruthenium red and 1.55 g of L-lysine acetate. After 20 min of fixation on ice, samples were centrifuged and washed twice in sodium cacodylate/ruthenium red buffer. Samples were then fixed for a second time for two hours with fixative that did not include the L-lysine acetate. Following two additional sodium cacodylate/ruthenium red buffer washes, samples were placed in 1% osmium tetroxide in sodium cacodylate/ruthenium red buffer for 1 h at room temperature. The fixed bacterial samples were then washed, dehydrated through a graded ethanol series and placed in 100% ethanol. The samples were infiltrated with a mixture of Eponate 12 resin (Ted Pella) and propylene oxide before being placed in pure Eponate 12 resin overnight. All resin-infiltrated bacterial samples were polymerized for 48 h in a 60 °C oven. The resin-embedded bacterial samples were sectioned to 70–80-nm-thick sections using a Leica UltraCut microtome (Leica Biosystems) and subsequently stained with 5% uranyl acetate and 2% lead citrate. The ultrathin sections were imaged with a JEOL JEM-1400 transmission electron microscope operated at 80 kV and equipped with a Gatan US1000 CCD camera.

Mice. WT C57BL/6J mice were purchased from The Jackson Laboratory and used at age 8–10 weeks. All experiments used age- and sex-matched mice. TKOs deficient in the gp91 component of the NADPH oxidase, lysozyme and CRAMP were derived by crossing *cybb*$^{-/-}$ (gp91; The Jackson Laboratory), *lysM*$^{-/-}$ (lysozyme; generously provided by D. Portnoy at the University of California, Berkeley) and *cramp*$^{-/-}$ (CRAMP; The Jackson Laboratory) mice. Mice were housed under specific pathogen-free conditions at Yerkes National Primate Center, Emory University. All experimental procedures were approved by the Emory University Institutional Animal Care and Use Committee. Mouse sample sizes were determined based on previous studies that generated highly statistically significant results while also minimizing the number of animals used (five mice per group for the majority of the experiments). Females were used for the majority of the animal experiments. Males were used in some experiments to match available knockout mice. Groups of mice with different genetic backgrounds had to be housed separately, precluding randomization and blinding.

Construction of the *ABUW_1645* (TetR) expression vector. To generate an expression plasmid for the *ABUW_1645* open reading frame, a 697-base pair (bp) DNA fragment, which began 60 bp upstream from the predicted *ABUW_1645* start codon and ended 82 bp downstream from the predicted *ABUW_1645* stop codon, was amplified by PCR using chromosomal DNA from

A. baumannii strain AB5075 as the template (Phusion Hot Start Polymerase; Thermo Fisher Scientific). Oligonucleotide primers (1645 Expression. 1.1; 5′ -GAGTGACGGCATGTCTATCT-3′ and 1645 Expression. 2.2; 5′-CTTATAGCCATAAGTGGTAATTGAG-3′) were treated with T4 Polynucleotide Kinase (New England Biolabs) to add 5′-phosphates before PCR amplification. The fragment was purified from an agarose gel slice and ligated using a Fast-Link Ligation Kit (Epicentre) into pWH1266 (ref. [36]) that had been digested with ScaI (New England Biolabs) and subsequently treated with shrimp alkaline phosphatase (New England Biolabs) to dephosphorylate the linearized vector. The ligation was transformed into *E. coli* TransforMax EC100D competent cells (Epicentre) and plated on LB with tetracycline (10 μg ml^{-1}) plates, resulting in the expression vector pKT1645.

RNA isolation and RNA-Seq analysis. Cultures of *A. baumannii* strain AB5075 VIR-O cells harbouring empty pWH1266 or pKT1645 and strain AB5075 AV-T cells harbouring empty pWH1266 or pKT1645 were grown in LB with tetracycline (5 μg ml^{-1}) at 37 °C with shaking to an optical density at a wavelength of 600 nm (OD_{600}) of ~0.75. The cells were harvested from cultures by centrifugation and RNA was isolated using a MasterPure RNA Purification Kit (Epicentre) according to the manufacturer's protocol. Contaminating DNA was removed by treatment using a TURBO DNA-free Kit (Ambion) according to the manufacturer's protocol. The RNA concentration was quantified using a NanoDrop ND-1000 spectrophotometer (Thermo Fisher Scientific). RNA purity was assessed by quantitative real-time PCR analysis of *clpX* expression in samples with or without reverse transcriptase.

RNA-Seq and analysis. RNA samples were first depleted of ribosomal RNAs using the Ribo-Zero rRNA Removal Kit (Illumina). RNA libraries were prepared using the NEBNext Ultra RNA Library Prep Kit for Illumina (New England Biolabs) and run on a single multiplexed HiSeq 4000 150PE lane (University of Maryland Genomics Resource Center). Paired-end Illumina libraries were mapped against the *A. baumannii* AB5075-UW genome using Bowtie aligner (version 0.12.9), and differential gene expression was quantified by DESeq (version 1.5.25) (University of Maryland Genomics Resource Center). The Fisher's exact test (modified by DESeq) was used to calculate the *P* values, which were adjusted for multiple testing by the Benjamini–Hochberg method. Differentially expressed transcripts with a *P* value of ≤0.05, a false discovery rate of ≤0.05 and a $\log_2$ fold change ≥1.7 were used. Sequence reads were deposited at the National Center for Biotechnology Information under BioProject PRJNA400082 as BioSamples SAMN07562376, SAMN07562377, SAMN07562378, SAMN07562379, SAMN07562380, SAMN07562381, SAMN07562382, SAMN07562383 and SAMN07562384.

Mouse pulmonary infection models. Approximately 5×10^7 colony-forming units (c.f.u.) at the 24 h time point and 5×10^8 c.f.u. at the 8 h time point were administered per mouse for infections to quantify the bacterial load, and approximately 3×10^8 c.f.u. were administered for the survival experiments. For mouse infections, overnight standing bacterial cultures at room temperature were subcultured in LB and grown at 37 °C with shaking to an OD_{600} of ~0.15, washed and then resuspended in PBS. Some 50 μl of bacterial inocula were inoculated intranasally to each mouse. Mice were anaesthetized with isoflurane immediately before intranasal inoculation. At each time point, the mice were sacrificed and the lungs, spleen and liver were harvested, homogenized and plated for c.f.u. on 0.5× LB plates.

Antimicrobial killing assays. An equal mixture of VIR-O and AV-T variants were grown to early-log phase in 2 ml LB or LB with tetracycline (5 μg ml^{-1}) for strains with plasmids. A 5 μl aliquot of each culture was mixed with 250 μl of 0.1× tryptone/yeast extract (1 g tryptone, 0.5 g yeast extract l^{-1}). Cells were mixed by vortexing and serial dilutions were plated on 0.5× LB agar plates to measure the initial c.f.u. values for both VIR-O and AV-T variants. Various antimicrobials were then added at the following final concentrations: CRAMP (10 μg ml^{-1}), lysozyme (10 mg ml^{-1}), LL-37 (15 μg ml^{-1}) and H_2O_2 (0.01%). Cells were treated for 1 h and dilutions were plated on 0.5× LB agar plates to enumerate the surviving VIR-O and AV-T variants.

Desiccation assay. Overnight standing bacterial cultures at room temperature were subcultured in LB and grown at 37 °C with shaking to an OD_{600} of ~0.15, washed and resuspended in PBS. Some 25 μl of bacterial inocula were desiccated on a 96-well flat-bottom polystyrene plate at room temperature. At each time point following desiccation, wells were rehydrated in 100 μl sterile PBS for 30 min, then serially diluted and plated for c.f.u. on 0.5× LB plates to enumerate the surviving VIR-O and AV-T variants.

Sensitivity to disinfectants. Overnight standing bacterial cultures at room temperature were subcultured in LB and grown at 37 °C with shaking to an OD_{600} of ~0.15. Culture (990 μl) was then added to tubes containing 10 μl of the appropriated disinfectants (BZT, BAK and CHG, respectively (all from Sigma–Aldrich)). Tubes were incubated at room temperature for 30 min. Cultures were then serially diluted and plated for c.f.u. enumerations.

Construction of an *ABUW_1645* deletion. Mutant *A. baumannii* strains were generated as previously described by ref. [37]. The *ABUW_1645* deletion was generated by PCR (Phusion Hot Start Polymerase; Thermo Fisher Scientific) amplification of approximately 2-kilobase-pair (kbp) up- and downstream fragments of the *ABUW_1645* gene using *A. baumannii* strain AB5075 genomic DNA as a template. Oligonucleotide primers 1645 Up-1.1 (AAAAAGGATCCCTACAGACCTTAAATAACGGTG) and 1645 Down-2.1 (AAAAAGGATCCTGGTCAAACTTTACGTGGT) were designed to contain BamHI restriction sites near the 5′ end and were paired with 1645 Up-2 (TGCTCTAAATGAAGCTTCTAA) and 1645 Down-1 (ATAATACTGTCCTAGATTAAAAATAAAAGC) primers, respectively. The up- and downstream fragments were gel purified (UltraClean 15 DNA Purification Kit; Mo Bio) and then ligated (Fast-Link DNA Ligation Kit; Epicentre) to produce an approximately 4-kbp deletion allele. This allele contained a deletion corresponding to amino acids 10–180 (92% of the protein sequence) of *ABUW_1645*. The *Δ1645* deletion allele was gel purified after ligation and re-amplified via PCR with 1645 Up-1.1 and Down-2.1 primers. The gel-purified *Δ1645* deletion allele and pEX18Tc were digested with BamHI and subsequently gel purified. Digested fragments were ligated and transformed into competent *E. coli* TransforMax EC100D cells (Epicentre). This ligation produced the suicide vector pΔ1645/EX18Tc.

To transfer the deletion allele to the chromosome of *A. baumannii* strain AB5075, suicide vector was electroporated into competent AB5075 cells that had been grown in LB medium and washed with 300 mM sucrose, as described by ref. [38]. Integrants were selected on LB with tetracycline (5 μg ml^{-1}). Counter-selection was carried out at room temperature on LB medium without sodium chloride supplemented with 10% sucrose. Potential mutants were screened by PCR amplification and confirmed by DNA sequencing.

An *ompR::Tc/Δ1645* double mutant was generated by transformation of the *Δ1645* mutant with chromosomal DNA from an *ompR::Tc* mutant obtained from the University of Washington strain collection.

Biofilm analysis. VIR-O and AV-T cells were taken directly from freezer stocks and grown in 2 ml 0.5× LB without shaking at room temperature to an OD_{600} of 0.1. Each tube was then used to inoculate 6 wells of a 96-well microtiter plate with 150 μl of culture. Plates were incubated stationary at 25 °C for 24 h. Cells were removed from each well and the OD_{600} was read for cell growth. To stain biofilms, 250 μl of 10% crystal violet was added to each well for 30 min. The crystal violet was gently decanted and each well was gently washed three times with distilled water. Some 300 μl of 33% acetic acid was added to each well to solubilize the crystal violet and this was then added to 600 μl 33% acetic acid. The absorbance of the sample was read at OD_{585}.

Growth of *A. baumannii*. The *A. baumannii* VIR-O and AV-T strains were subcultured to an OD_{600} of 0.03 in Chamberlain's Medium (Teknova), LB (BD Biosciences) or minimal media (M9) supplemented with 0.2% casamino acids. The iron chelator, 2,2′-dipyridyl disulphide (156 μM) was added as indicated. Subcultures were placed at 37 °C with aeration in a BioTek Synergy Mx Microplate Reader (Applied Biosystems) and the OD_{600} was measured every 30 min for 20 h.

Statistics. Statistical analyses were performed using Prism 5 (https://www.graphpad.com/; GraphPad Software). The significance of the mouse experiments was determined by Mann–Whitney test, as not all data were normally distributed. All in vitro experiments were analysed using a two-tailed unpaired student's *t*-test (for data with a normal distribution). All experiments were repeated at least two to three times. All replicates shown are biological replicates.

Reporting Summary. Further information on experimental design is available in the Nature Research Reporting Summary linked to this article.

Data availability. All data supporting this study are available from the corresponding authors upon request. Compiled RNA-Seq data are available in Supplementary Table 1. Sequence reads have been deposited at the National Center for Biotechnology Information under BioProject PRJNA400082 as BioSamples SAMN07562376, SAMN07562377, SAMN07562378, SAMN07562379, SAMN07562380, SAMN07562381, SAMN07562382, SAMN07562383 and SAMN07562384.

Received: 29 September 2017; Accepted: 22 March 2018;
Published online: 23 April 2018

References

1. O'Neill, J. *Antimicrobial Resistance: Tackling a Crisis for the Health and Wealth of Nations* (UK Government & Wellcome Trust, 2014); https://amr-review.org/sites/default/files/AMR%20Review%20Paper%20-%20Tackling%20a%20crisis%20for%20the%20health%20and%20wealth%20of%20nations_1.pdf
2. Bergogne-Berezin, E. & Towner, K. J. *Acinetobacter* spp. as nosocomial pathogens: microbiological, clinical, and epidemiological features. *Clin. Microbiol. Rev.* **9**, 148–165 (1996).

3. Antunes, L. C., Visca, P. & Towner, K. J. *Acinetobacter baumannii*: evolution of a global pathogen. *Pathog. Dis.* **71**, 292–301 (2014).
4. Dijkshoorn, L., Nemec, A. & Seifert, H. An increasing threat in hospitals: multidrug-resistant *Acinetobacter baumannii*. *Nat. Rev. Microbiol.* **5**, 939–951 (2007).
5. Joly-Guillou, M. L. Clinical impact and pathogenicity of *Acinetobacter*. *Clin. Microbiol. Infect.* **11**, 868–873 (2005).
6. Murray, C. K. & Hospenthal, D. R. *Acinetobacter* infection in the ICU. *Crit. Care Clin.* **24**, 237–248 (2008).
7. Charnot-Katsikas, A. et al. Two cases of necrotizing fasciitis due to *Acinetobacter baumannii*. *J. Clin. Microbiol.* **47**, 258–263 (2009).
8. Guerrero, D. M. et al. *Acinetobacter baumannii*-associated skin and soft tissue infections: recognizing a broadening spectrum of disease. *Surg. Infect.* **11**, 49–57 (2010).
9. Lowman, W., Kalk, T., Menezes, C. N., John, M. A. & Grobusch, M. P. A case of community-acquired *Acinetobacter baumannii* meningitis—has the threat moved beyond the hospital? *J. Med. Microbiol.* **57**, 676–678 (2008).
10. Telang, N. V., Satpute, M. G., Dhakephalkar, P. K., Niphadkar, K. B. & Joshi, S. G. Fulminating septicemia due to persistent pan-resistant community-acquired metallo-beta-lactamase (IMP-1)-positive *Acinetobacter baumannii*. *Indian J. Pathol. Microbiol.* **54**, 180–182 (2011).
11. Boucher, H. W. et al. Bad bugs, no drugs: no ESKAPE! An update from the Infectious Diseases Society of America. *Clin. Infect. Dis.* **48**, 1–12 (2009).
12. Doi, Y., Husain, S., Potoski, B. A., McCurry, K. R. & Paterson, D. L. Extensively drug-resistant *Acinetobacter baumannii*. *Emerg. Infect. Dis.* **15**, 980–982 (2009).
13. Gottig, S. et al. Detection of pan drug-resistant *Acinetobacter baumannii* in Germany. *J. Antimicrob. Chemother.* **69**, 2578–2579 (2014).
14. Lei, J. et al. Extensively drug-resistant *Acinetobacter baumannii* outbreak cross-transmitted in an intensive care unit and respiratory intensive care unit. *Am. J. Infect. Control* **44**, 1280–1284 (2016).
15. Park, Y. K. et al. Extreme drug resistance in *Acinetobacter baumannii* infections in intensive care units, South Korea. *Emerg. Infect. Dis.* **15**, 1325–1327 (2009).
16. Maragakis, L. L. & Perl, T. M. *Acinetobacter baumannii*: epidemiology, antimicrobial resistance, and treatment options. *Clin. Infect. Dis.* **46**, 1254–1263 (2008).
17. Villegas, M. V. & Hartstein, A. I. *Acinetobacter* outbreaks, 1977–2000. *Infect. Control Hosp. Epidemiol.* **24**, 284–295 (2003).
18. Fernandez-Cuenca, F. et al. Reduced susceptibility to biocides in *Acinetobacter baumannii*: association with resistance to antimicrobials, epidemiological behaviour, biological cost and effect on the expression of genes encoding porins and efflux pumps. *J. Antimicrob. Chemother.* **70**, 3222–3229 (2015).
19. Jawad, A., Seifert, H., Snelling, A. M., Heritage, J. & Hawkey, P. M. Survival of *Acinetobacter baumannii* on dry surfaces: comparison of outbreak and sporadic isolates. *J. Clin. Microbiol.* **36**, 1938–1941 (1998).
20. Hassan, K. A. et al. Transcriptomic and biochemical analyses identify a family of chlorhexidine efflux proteins. *Proc. Natl Acad. Sci. USA* **110**, 20254–20259 (2013).
21. Brooks, S. E., Walczak, M. A., Hameed, R. & Coonan, P. Chlorhexidine resistance in antibiotic-resistant bacteria isolated from the surfaces of dispensers of soap containing chlorhexidine. *Infect. Control Hosp. Epidemiol.* **23**, 692–695 (2002).
22. Jacobs, A. C. et al. AB5075, a highly virulent isolate of *Acinetobacter baumannii*, as a model strain for the evaluation of pathogenesis and antimicrobial treatments. *mBio* **5**, e01076–14 (2014).
23. Tipton, K. A., Dimitrova, D. & Rather, P. N. Phase-variable control of multiple phenotypes in *Acinetobacter baumannii* strain AB5075. *J. Bacteriol.* **197**, 2593–2599 (2015).
24. Geisinger, E. & Isberg, R. R. Antibiotic modulation of capsular exopolysaccharide and virulence in *Acinetobacter baumannii*. *PLoS Pathog.* **11**, e1004691 (2015).
25. Martin, T. R. & Frevert, C. W. Innate immunity in the lungs. *Proc. Am. Thorac. Soc.* **2**, 403–411 (2005).
26. Hiemstra, P. S., McCray, P. B. Jr & Bals, R. The innate immune function of airway epithelial cells in inflammatory lung disease. *Eur. Respir. J.* **45**, 1150–1162 (2015).
27. Tipton, K. A. & Rather, P. N. An *ompR–envZ* two-component system ortholog regulates phase variation, osmotic tolerance, motility, and virulence in *Acinetobacter baumannii* strain AB5075. *J. Bacteriol.* **199**, e00705-16 (2016).
28. Tipton, K. A., Farokhyfar, M. & Rather, P. N. Multiple roles for a novel RND-type efflux system in *Acinetobacter baumannii* AB5075. *MicrobiologyOpen* **6**, e00418 (2016).
29. Regeimbal, J. M. et al. Personalized therapeutic cocktail of wild environmental phages rescues mice from *Acinetobacter baumannii* wound infections. *Antimicrob. Agents Chemother.* **60**, 5806–5816 (2016).
30. Slutsky, B. et al. "White–opaque transition": a second high-frequency switching system in *Candida albicans*. *J. Bacteriol.* **169**, 189–197 (1987).
31. Turner, K. H., Vallet-Gely, I. & Dove, S. L. Epigenetic control of virulence gene expression in *Pseudomonas aeruginosa* by a LysR-type transcription regulator. *PLoS Genet.* **5**, e1000779 (2009).
32. Diard, M. et al. Stabilization of cooperative virulence by the expression of an avirulent phenotype. *Nature* **494**, 353–356 (2013).
33. Ronin, I., Katsowich, N., Rosenshine, I. & Balaban, N. Q. A long-term epigenetic memory switch controls bacterial virulence bimodality. *eLife* **6**, e19599 (2017).
34. Mouammine, A. et al. An antimicrobial peptide-resistant minor subpopulation of *Photorhabdus luminescens* is responsible for virulence. *Sci. Rep.* **7**, 43670 (2017).
35. Bommanavar, S. B., Gugwad, S. & Malik, N. Phenotypic switch: the enigmatic white–gray–opaque transition system of *Candida albicans*. *J. Oral. Maxillofac. Pathol.* **21**, 82–86 (2017).
36. Hunger, M., Schmucker, R., Kishan, V. & Hillen, W. Analysis and nucleotide sequence of an origin of DNA replication in *Acinetobacter calcoaceticus* and its use for *Escherichia coli* shuttle plasmids. *Gene* **87**, 45–51 (1990).
37. Hoang, T., Karkhoff-Schweizer, R., Kutchma, A. & Schweizer, H. A broad-host-range Flp-*FRT* recombination system for site-specific excision of chromosomally-located DNA sequences: application for isolation of unmarked *Pseudomonas aeruginosa* mutants. *Gene* **212**, 77–86 (1998).
38. Choi, K. & Schweizer, H. mini-Tn7 insertion in bacteria with single *att*Tn7 sites: example *Pseudomonas aeruginosa*. *Nat. Protoc.* **1**, 153–161 (2006).

Acknowledgements

The authors thank staff at the Genomics Resource Center at the University of Maryland for help with RNA-Seq and analysis, H. Ratner for the mice experiments, D. Bonenberger for breeding the knockout mice and W. Shafer for comments on the manuscript. This study was supported in part by the Robert P. Apkarian Integrated Electron Microscopy Core, which is subsidized by the Emory College of Arts and Sciences and the Emory University School of Medicine, and is one of the Emory Integrated Core Facilities. Additional support was provided by the Georgia Clinical and Translational Science Alliance of the National Institutes of Health (NIH) under award number UL1TR000454. P.N.R is supported by NIH grants R21AI115183 and R01072219, VA Merit award I01 BX001725 and a Research Career Scientist Award from the Department of Veterans Affairs. D.S.W. is supported by a Burroughs Wellcome Fund Investigators in the Pathogenesis of Infectious Disease award, VA Merit award I01 BX002788 and NIH grant AI098800. This content is solely the responsibility of the authors and does not necessarily represent the official views of the NIH and Department of Veterans Affairs.

Author contributions

C.Y.C., K.A.T. and M.F. conducted the experiments. C.Y.C., K.A.T., D.S.W. and P.N.R prepared the manuscript. E.M.B. provided the samples from human patients. D.S.W. and P.N.R. planned and directed the study.

Competing interests

The authors declare no competing interests.

Additional information

Supplementary information is available for this paper at https://doi.org/10.1038/s41564-018-0151-5.

Reprints and permissions information is available at www.nature.com/reprints.

Correspondence and requests for materials should be addressed to D.S.W. or P.N.R.

Publisher's note: Springer Nature remains neutral with regard to jurisdictional claims in published maps and institutional affiliations.

nature research

Corresponding author(s): Philip Rather, David Weiss

☐ Initial submission ☒ Revised version ☐ Final submission

Life Sciences Reporting Summary

Nature Research wishes to improve the reproducibility of the work that we publish. This form is intended for publication with all accepted life science papers and provides structure for consistency and transparency in reporting. Every life science submission will use this form; some list items might not apply to an individual manuscript, but all fields must be completed for clarity.

For further information on the points included in this form, see Reporting Life Sciences Research. For further information on Nature Research policies, including our data availability policy, see Authors & Referees and the Editorial Policy Checklist.

Experimental design

1. Sample size

Describe how sample size was determined.

Sample size was reported in the figure legends.

For mouse studies, statistical significance was determined using the Mann-Whitney test (n≥4). To protect animal welfare, a minimal number of animals were used (5 mice were used per group for the majority of experiments).

For in vitro studies, statistical significance was determined using the two-tailed student's t-test (n≥2), and 3 replicates per condition were used in the majority of in vitro experiments.

To determine VIR-O and AV-T switching frequencies, a minimum of 6 colonies for each strain was tested.

For biofilm assays, 6 individual wells per strain were used and repeated experiments gave consistently reproducible results.

For the electron microscopy to visualize capsule, a representative image was shown. Multiple images shown similar differences.

Growth curves were repeated at least three times and a representative experiment was shown for each.

2. Data exclusions

Describe any data exclusions.

N/A, no data has been excluded.

3. Replication

Describe whether the experimental findings were reliably reproduced.

All the experiments were reliably reproduced.

4. Randomization

Describe how samples/organisms/participants were allocated into experimental groups.

There was no randomization in the animal experiments.
The mouse groups used in this study were age- and gender-matched, housed in the same facility or purchased directly from Jackson Laboratory (Bar Harbor, Maine). Thus, the mouse groups were equivalent (other than genotype) at the start of experiments. Therefore any differences observed within groups were attributable to the infecting bacterial strains or genotype of the mice.

5. Blinding

Describe whether the investigators were blinded to group allocation during data collection and/or analysis.

No blinding was performed for animal studies.
The mouse groups used in this study were age- and gender-matched, housed in

the same facility or purchased directly from Jackson Laboratory (Bar Harbor, Maine). Thus, the mouse groups were equivalent (other than genotype) at the start of experiments. Therefore any differences observed within groups were attributable to the infecting bacterial strains or genotype of the mice.

Note: all studies involving animals and/or human research participants must disclose whether blinding and randomization were used.

6. Statistical parameters

For all figures and tables that use statistical methods, confirm that the following items are present in relevant figure legends (or in the Methods section if additional space is needed).

n/a	Confirmed
☐	☒ The exact sample size (*n*) for each experimental group/condition, given as a discrete number and unit of measurement (animals, litters, cultures, etc.)
☐	☒ A description of how samples were collected, noting whether measurements were taken from distinct samples or whether the same sample was measured repeatedly
☐	☒ A statement indicating how many times each experiment was replicated
☐	☒ The statistical test(s) used and whether they are one- or two-sided (note: only common tests should be described solely by name; more complex techniques should be described in the Methods section)
☒	☐ A description of any assumptions or corrections, such as an adjustment for multiple comparisons
☐	☒ The test results (e.g. *P* values) given as exact values whenever possible and with confidence intervals noted
☐	☒ A clear description of statistics including central tendency (e.g. median, mean) and variation (e.g. standard deviation, interquartile range)
☐	☒ Clearly defined error bars

See the web collection on statistics for biologists for further resources and guidance.

Software

Policy information about availability of computer code

7. Software

Describe the software used to analyze the data in this study.	Statistical analyses were performed using Prism 5 ver 5.0 (GraphPad Software). No custom codes were used.

For manuscripts utilizing custom algorithms or software that are central to the paper but not yet described in the published literature, software must be made available to editors and reviewers upon request. We strongly encourage code deposition in a community repository (e.g. GitHub). *Nature Methods* guidance for providing algorithms and software for publication provides further information on this topic.

Materials and reagents

Policy information about availability of materials

8. Materials availability

Indicate whether there are restrictions on availability of unique materials or if these materials are only available for distribution by a for-profit company.	No restrictions and no unique materials were used.

9. Antibodies

Describe the antibodies used and how they were validated for use in the system under study (i.e. assay and species).	N/A. No antibodies were used.

10. Eukaryotic cell lines

a. State the source of each eukaryotic cell line used.	No eukaryotic cell lines were used.
b. Describe the method of cell line authentication used.	N/A
c. Report whether the cell lines were tested for mycoplasma contamination.	N/A
d. If any of the cell lines used are listed in the database of commonly misidentified cell lines maintained by ICLAC, provide a scientific rationale for their use.	N/A

Animals and human research participants

Policy information about studies involving animals; when reporting animal research, follow the ARRIVE guidelines

11. Description of research animals

Provide details on animals and/or animal-derived materials used in the study.

Wild-type C57BL/6J mice were purchased from Jackson Laboratories and used at age 8-10 weeks; all experiments used age- and sex-matched mice. All the knockout mice used in this study were generated in the C57BL/6J mice background.

Policy information about studies involving human research participants

12. Description of human research participants

Describe the covariate-relevant population characteristics of the human research participants.

N/A. No human research participants were involved.